INFLUENCE OF CRACKING ON THE SEISMIC RESPONSE OF CONCRETE GRAVITY DAMS

D. Wepf (I)
P. Skrikerud (II)
H. Bachmann (III)

Presenting Author: D. Wepf

SUMMARY

The response of seismically loaded, unreinforced concrete gravity dams is studied taking account of initiation, extension, closing and reopening of discrete cracks. The aim of the present work is to develop models and computational procedures suited for the numerical approximation of these physical events and for the determination of their influence on the response of the concrete structure. For this aim a computer program based on the finite-element method is developed. The program is, at present, restricted to two-dimensional structures under plane-stress conditions. The response of two concrete gravity dams to horizontal earthquake excitation is examined. In general, larger displacements but smaller stresses result when compared with a similar calculation which does not allow for cracking.

INTRODUCTION

The behavior of concrete dams due to seismic loading is a matter of public concern because the impounded water, in case of a dam failure, represents a severe threat to the environment. One important parameter for the safety of concrete dams under seismic loading is the non-linear cracking phenomenon occurring when the tensile strength of the material is exceeded. To study the effects of this physical event on the response of the structure, a two-dimensional computer program, based on the discrete crack formulation in a finite element mesh, is developed. First applications of this program are presented here.

COMPUTATIONAL PROCEDURE

The concrete structure is described using bilinear, quadrilateral or triangular, isoparametric finite elements under plane stress conditions. The discrete crack formulation involves the separation of adjacent elements, introducing additional nodal points and hence new degrees of freedom. The associated numerical problems (increased bandwidth of the structural matrices) are avoided through the selection of an explicit integration procedure for the equations of motion (Ref. 1).

(I) Research Assistant, Institute of Structural Engineering, Swiss Federal Institute of Technology, Zürich

(II) Engineering Consultant, Structural Engineering AS, Oslo, Norway

(III) Professor of Civil Engineering, Institute of Structural Engineering, Swiss Federal Institute of Technology, Zürich

Initiation and extension of cracks

For the initiation of a crack, the equivalent tensile strength criterion based on the approximated biaxial failure condition of concrete (Ref. 2) is applied. As long as one of the principal stresses is a tensile stress, cracking of the concrete is assumed. At present, the same procedure is also used for the extension of cracks even though the discrete crack formulation is suited for alternative approaches. For the dynamic response of concrete structures, reliable and economically feasible methods for the modeling of discrete crack propagation are controversional.

To achieve a relatively simple algorithm, it is assumed that the crack initiates from the node of the outer surface of the structure which is next to the governing integration point (node A, Fig. 1). Further, it is presumed that the crack will propagate perpendicularly to the principal tensile stress through the entire element to point E. This direction, represented by the angle θ, does normally not coincide with the original element mesh. Therefore, in order to allow for crack propagation along inter-element boundaries, the mesh is updated either through distortion (node C is moved to E, Fig. 1a) or combined distortion and division (node D is moved to E and the quadrilateral element i divided into the triangular elements i and i', Fig. 1b). In subsequent time steps, new cracks develop in the same manner whereby already existing cracks represent an extension to the outer boundary of the structure.

The structural properties associated with node A in the original mesh are henceforth split between A and A'. Before continuing the temporal integration, the crack width as well as the shear deformation are equated to zero so that the new node A' initially is given the same amount of displacement as A. Moreover, the displacements, velocities and accelerations of point E are recalculated according to the inter-element shape functions. When cracks close, the hypothesis of a perfectly plastic impact is assumed to apply for the determination of the motion of the nodes involved. A closed crack reopens as soon as a net tensile stress develops across the crack.

Crack element

Between elements separated by a crack, so-called crack elements are introduced. These model the roughness of the crack surface and serve to determine the stress transfer by aggregate interlock resulting from relative displacements of the two crack surfaces. According to tests, the crack width, the maximum aggregate size and the loading history are important parameters for the stress transfer.

The crack width is the governing factor for the apparent stiffness and load transfer capacity. It is modeled, as shown in Fig. 2, with a set of parallel springs representing layers of the crack surface. The number of springs n and the maximum width y_{max}, for which contact still can be achieved, are determined through type and size of the aggregate. For a specific relative displacement u and a specific crack width w, a certain number of springs m are activated (Fig. 3). Thus, through an adequate choice of all the spring stiffnesses, crack-width dependent shear transmission can be modeled. For the results presented here all crack-width dependent numerical values are determined according to a procedure valid for initial loading (Ref. 3).

The influence of the loading history for each individual spring is approximated as indicated in the stress-displacement relationship of Fig. 4. As the

unloading stiffness is larger than both the initial and the reloading stiffnesses, a permanent shear displacement, which in general will be different for each spring of the crack element, will result.

Two conditions for the closure of a crack are incorporated. The first, namely the crack width w less than or equal to zero, is obvious. The second condition is a function of the remaining shear deformations and equivalent layer thicknesses of the springs, and the decreasing crack width and the relative displacement u of the crack surface (Ref. 1). The crack element closes as soon as one of the conditions applies.

Interaction with adjacent media

To demonstrate the basic features of the crack algorithm, some computations are performed neglecting the fluid-structure and the soil-structure interaction. With these calculations as a reference, simplified approximations to the interaction phenomena applicable to the time domain are introduced in order to assess their influence on the cracking behavior.

Westergaard (Ref. 4) developed a basic concept of representing the effect of the reservoir on the earthquake response of a gravity dam. This formulation is frequently used in the seismic analysis of such dams. For that reason and in spite of its limiting assumptions, the approximate added mass concept, which is the usual way of representing the Westergaard solution, is adopted here. The most important assumptions of this formulation are a rigid dam with a vertical upstream face, two-dimensional modeling of the structure, incompressible fluid, a reservoir which extends to infinity (radiation damping), neglecting of surface waves (lower frequency bound), and excitation frequencies lower than the fundamental frequency of the reservoir (upper frequency bound).

The flexibility of the soil is approximated with frequency-independent linear springs and viscous dampers (dashpots). The expressions for a rigid strip foundation located on the top of an elastic half plane are derived in Ref. 5. The horizontal stiffness and damping coefficients are evenly distributed between the foundation nodes. The vertical springs and dampers introduced at the foundation nodes represent both vertical and rocking motions. A distribution of the vertical springs which accurately simulates the correct stiffness of both is not possible. In the analyses described here, the rocking stiffness is deemed more important and therefore modeled exactly, whereas for the vertical stiffness twice the theoretical value results.

APPLICATIONS

To test the algorithm described above, two specific types of concrete gravity dams are analized. As the aim of the analyses is to assess the influence of the different parameters on the response, the cross-sections are somewhat simplified. Cross-section Type A, similar to the Koyna dam, with a relatively large mass at the top is shown in Fig. 5. It is selected for calculation because it is one of the few dams where seismic cracking is reported (e.g. Ref. 6). The other one, Type B (Fig. 6), is a typical triangular cross-section which is frequently found in the Swiss Alps. Its special characteristic is the considerable height of almost 300 m. For both types, the material constants as well as the finite element mesh are indicated in the figures. In contrast to reality, the material constants are assumed to be valid for the entire structure. In addition, neither mutual interaction of adjacent blocks nor any effect of construction joints are considered. The element mesh is chosen arbi-

trarily. If nothing else is specified the structures are assumed rigidly supported at the base. The earthquake excitation is approximated with the horizontal time history of figure 7, scaled to the approximate maximum acceleration value. Synchronous excitation (vertically propagating waves) is assumed. For the present study, no vertical excitation is considered.

Figure 8 shows the development of the crack pattern for Type A at selected time steps. The first crack initiates near the fixed base on the upstream side. At a later stage, when the upper part of the cross-section moves to the left, the second crack sequence is formed near the point of discontinuity. In subsequent movements cracks are extending from this point, and they finally reach the upstream face. Type B (Fig. 9) shows a somewhat different behavior. During the first larger movement of the dam to the left, caused by the first three pulses of the acceleration time history, the cracks propagate through the structure leaving an upper part isolated. In the following oscillation to the opposite side, a crack in the lower part of the upstream face develops. Figures 8 and 9 demonstrate that the overall crack patterns of the two types are similar. For comparison, the final crack pattern of Type A for an empty reservoir is depicted in figure 10a. In contrast to the case with a full reservoir, no cracks on the upstream side result, and hence no penetration of the cross-section takes place. Figure 10 also gives an indication of the influence of the aggregate interlock phenomenon. For the overall results including crack pattern the consequences of crack element modeling seem to be minor. Also for Type B (Fig. 11), no crack occurs in the lower part of the upstream face for the empty reservoir. The upper cracks, however, still penetrate the cross section, and this even occurs at an earlier stage of the time history. Figure 12 shows a comparison of the horizontal displacement at the dam crest between a non-linear calculation which allows for cracking and a linear one which does not. The crest undergoes larger displacements when cracking occurs, and also the apparent period of the oscillation is somewhat increased. In figure 13, the same comparison is carried out for the maximum principal stresses. The stresses are taken from an element near a crack. After the crack has developed, the tensile stresses f_t are, of course, noticeably reduced. The consideration of soil-structure interaction generally reduces the amount of cracks in the structure, when the ratio of Young's modulus of the foundation E_f to Young's modulus of the structure E_s is lowered. The overall displacements, however, normally increase (Fig. 14). In figure 15, finally, the influence of the reservoir on the horizontal displacements is demonstrated. For the case of Type A the reservoir water leads to a larger apparent period and to larger displacements. Despite the complete separation of the upper part of the structure no collapse of the dam results.

CONCLUSIONS

Both types of dams examined here experience cracking for appropriate values of the parameters. However, the influence of certain parameters on the response is different for the two types. It is found that seismic cracking does not necessarily lead to a collapse of the dam. In general, larger displacements but smaller stresses result as compared to a calculation which does not allow for seismic cracking. Based on the experience gained so far with the algorithm selected, further studies with refined modeling of the adjacent media should be done.

ACKNOWLEDGEMENTS

This research was carried out with the financial support of the Swiss Federal Office for Water Management. The authors express their sincere thanks and appreciation for this support. Thanks are also given to M. Hohberg for help in calculation of the samples.

REFERENCES

1. Skrikerud P, 'Models and computational procedures for the cracking behavior of seismically loaded unreinforced concrete structures', Ph. D. Thesis, Swiss Federal Institute of Technology, Zürich, 1982. (In German)
2. Tasuji ME et al., 'Biaxial stress-strain relationship for concrete', Magazine of Concrete Res., 31 (1979).
3. Bazant ZP, Gambarova P, 'Rough cracks in reinforced concrete', J. Struct. Div., ASCE, 106 (1980).
4. Westergaard HM, 'Water pressures on dams during earthquakes', Proc. ASCE, 57 (1931) and Trans. ASCE, 98 (1933).
5. Luco JE, Westmann RA, 'Dynamic response of a rigid footing bonded to an elastic half-plane', J. App. Mech., ASME, 39 (E2) (1972).
6. Jaini et al., 'Behavior of Koyna Dam - Dec. 11, 1967 earthquake', J. Struct. Div., ASCE, 98 (1972).

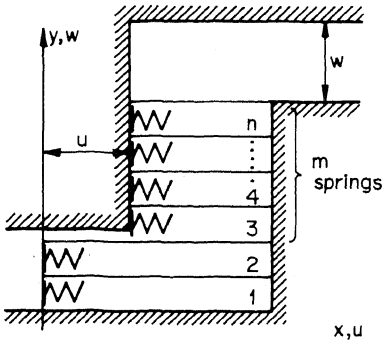

Fig. 3: Partial activation of springs

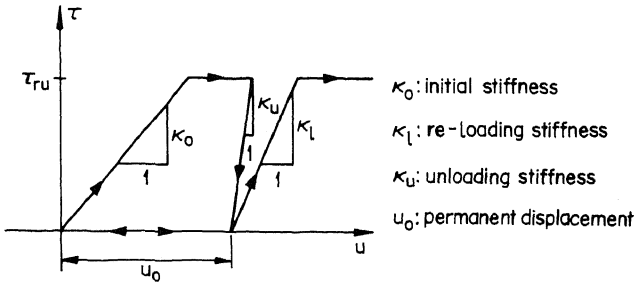

Fig. 4: Stress-displacement relationship of individual spring

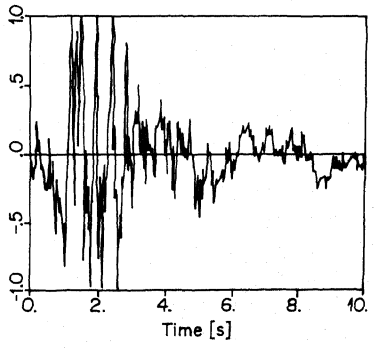

Fig. 7: Horizontal acceleration time history (normalized)

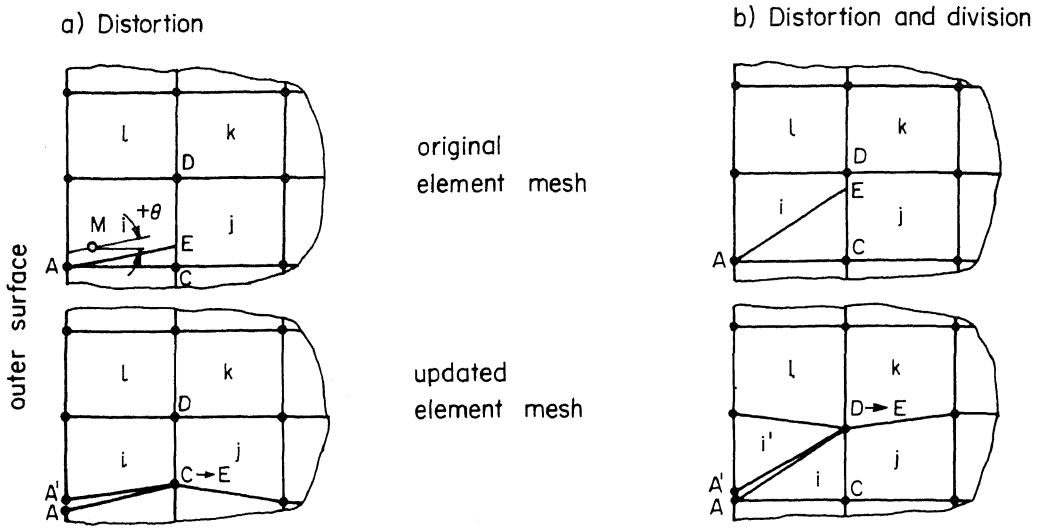

Fig. 1 : Modification of the FE-mesh by a new crack (M: Gauss integration point)

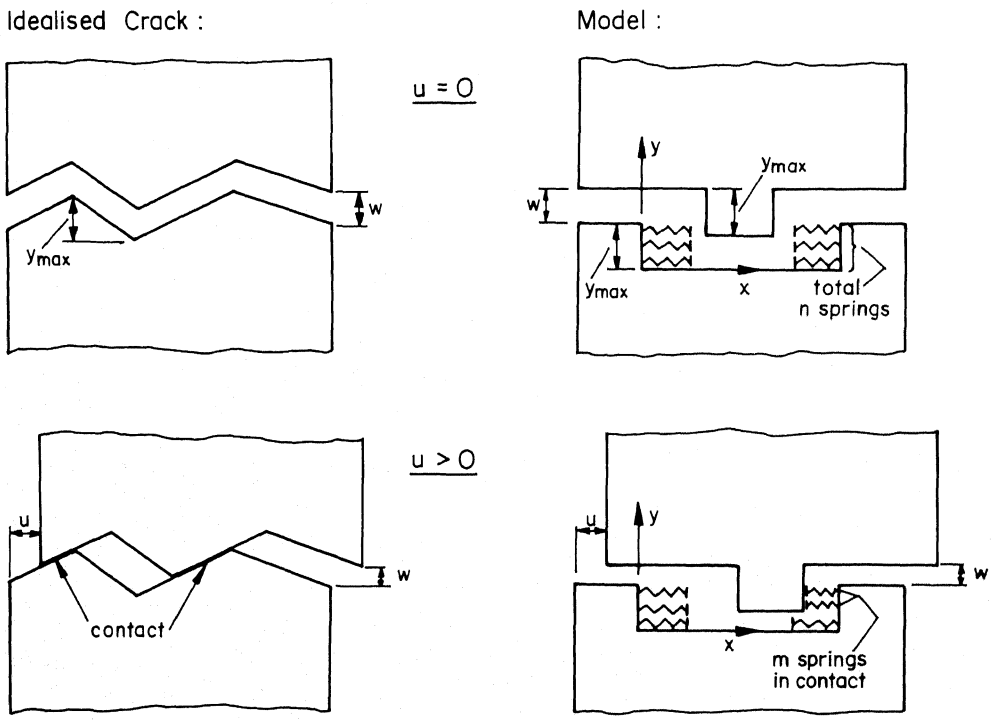

Fig. 2 : Modelling of crack surface with parallel springs

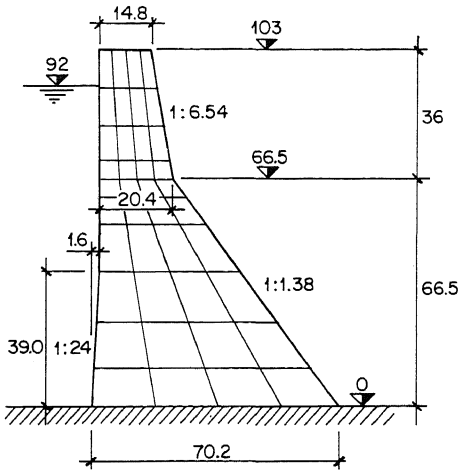

Fig. 5: Cross section, Type A.

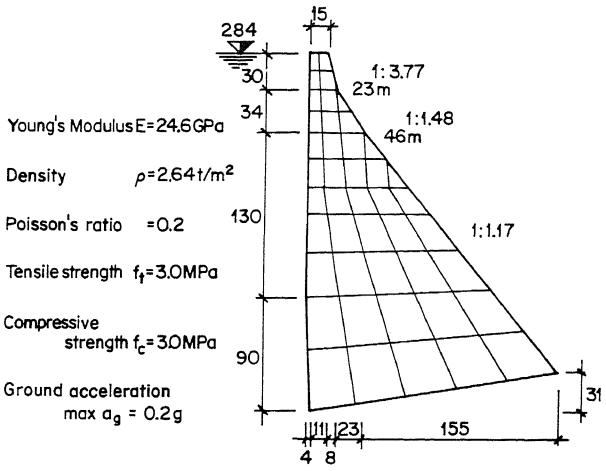

Fig. 6: Cross section, Type B.

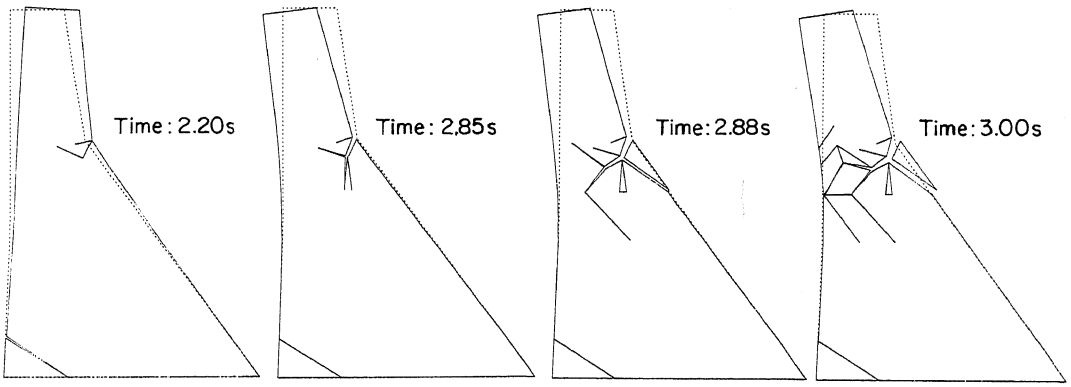

Fig. 8: Crack development, Type A, reservoir full.

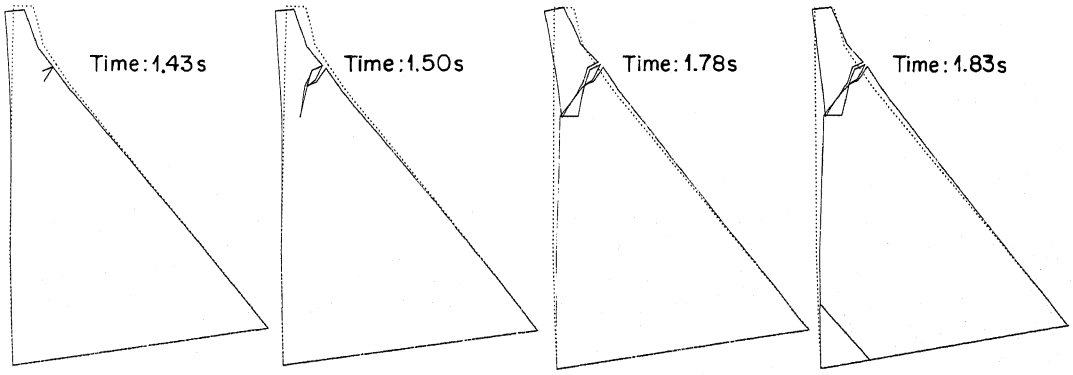

Fig. 9: Crack development, Type B, reservoir full.

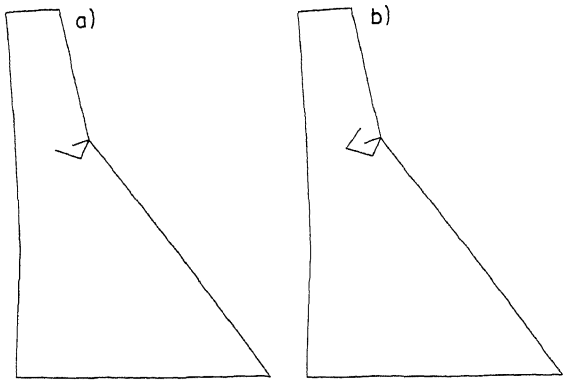

Fig.10: Final crack pattern, Type A, reservoir empty.
a) with b) without aggregate interlock.

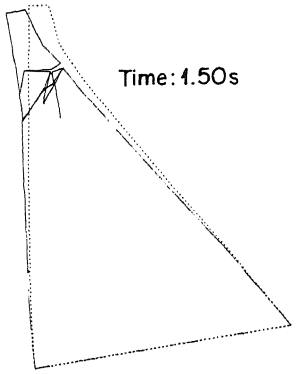

Fig. 11: Crack pattern, Type B, reservoir empty.

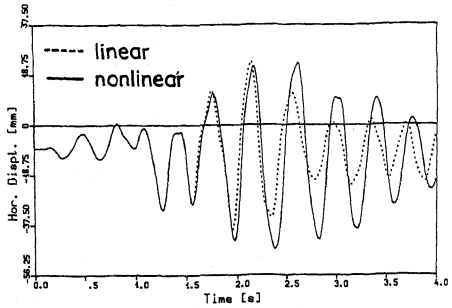

Fig.12: Displacements of crest, Type A, reservoir empty.

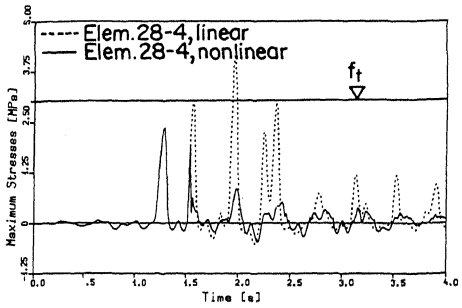

Fig.13: Maximum principal stress, Type A, reservoir empty.

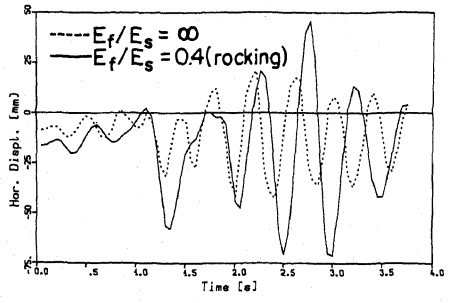

Fig.14: Displacements of crest, Type A, reservoir empty.

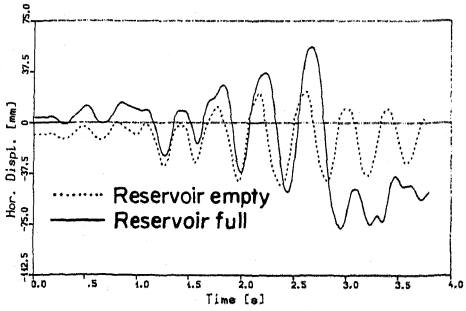

Fig.15: Displacements of crest Type A.